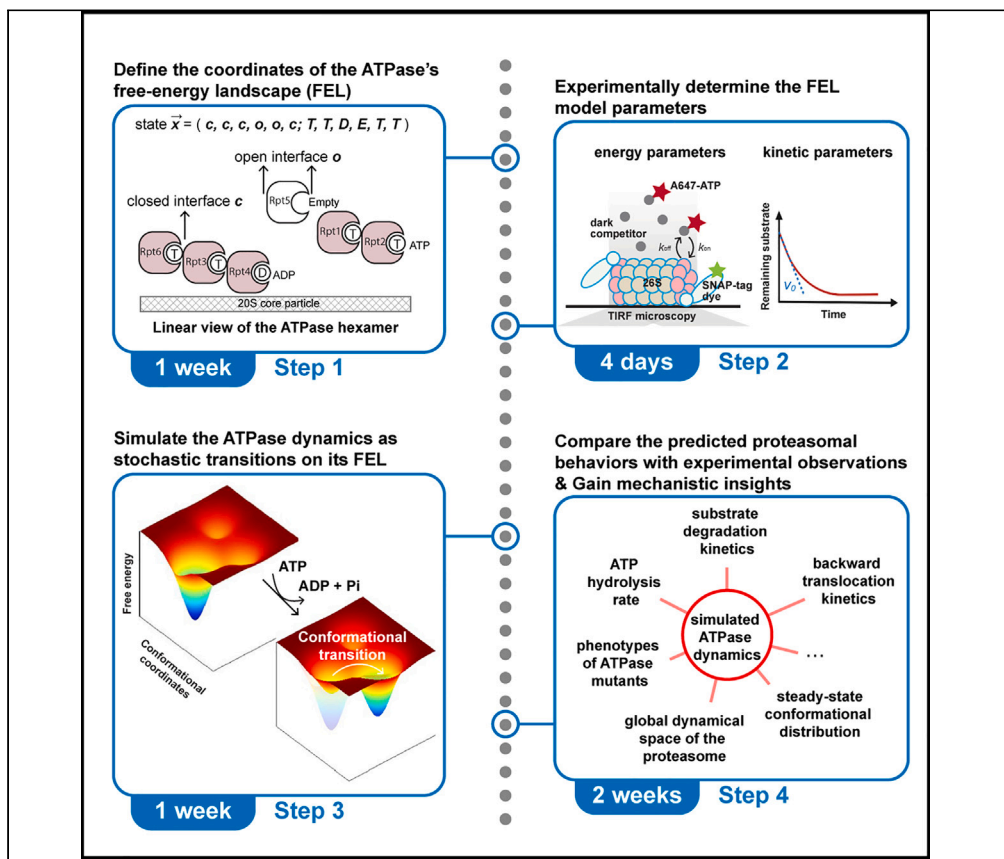


## Protocol

# Simulating the conformational dynamics of the ATPase complex on proteasome using its free-energy landscape



Rui Fang, Ying Lu

ruifang@fas.harvard.edu  
(R.F.)

ying\_lu@hms.harvard.edu  
(Y.L.)

### Highlights

A procedure to simulate the dynamics of the ATPase complex on proteasome

We first empirically determine the free-energy landscape (FEL) of the ATPase complex

We simulate the ATPase dynamics as stochastic transitions on its FEL

We map ATPase's global dynamics to understand the mechanism of protein degradation

The AAA+ ATPase complex on proteasome powers its functions through a series of intricate conformational transitions. Here, we describe a procedure to simulate the conformational dynamics of the proteasomal ATPase complex. We first empirically determined the free-energy landscape (FEL) of proteasome and then simulated proteasome's conformational changes as stochastic transitions on its FEL. We compared the FEL-predicted proteasomal behaviors with experimental measurements and analyzed the map of the ATPase's global dynamics to gain mechanistic insights into proteasomal degradation.

Publisher's note: Undertaking any experimental protocol requires adherence to local institutional guidelines for laboratory safety and ethics.

Fang & Lu, STAR Protocols 4, 102182

December 15, 2023 © 2023

The Author(s).

<https://doi.org/10.1016/j.xpro.2023.102182>

j.xpro.2023.102182



## Protocol

## Simulating the conformational dynamics of the ATPase complex on proteasome using its free-energy landscape

Rui Fang<sup>1,2,3,\*</sup> and Ying Lu<sup>1,4,\*</sup><sup>1</sup>Department of Systems Biology, Harvard Medical School, Boston, MA 02115, USA<sup>2</sup>Department of Molecular and Cellular Biology, Harvard University, Cambridge, MA 02138, USA<sup>3</sup>Technical contact<sup>4</sup>Lead contact\*Correspondence: [rui.fang@fas.harvard.edu](mailto:rui.fang@fas.harvard.edu) (R.F.), [ying.lu@hms.harvard.edu](mailto:ying.lu@hms.harvard.edu) (Y.L.)<https://doi.org/10.1016/j.xpro.2023.102182>

## SUMMARY

The AAA+ ATPase complex on proteasome powers its functions through a series of intricate conformational transitions. Here, we describe a procedure to simulate the conformational dynamics of the proteasomal ATPase complex. We first empirically determined the free-energy landscape (FEL) of proteasome and then simulated proteasome's conformational changes as stochastic transitions on its FEL. We compared the FEL-predicted proteasomal behaviors with experimental measurements and analyzed the map of the ATPase's global dynamics to gain mechanistic insights into proteasomal degradation.

For complete details on the use and execution of this protocol, please refer to Fang et al. (2022).<sup>1</sup>

## BEFORE YOU BEGIN

## Introduction

The ring-shaped oligomeric ATPases control key biological processes including protein folding, transcription, DNA replication, cellular cargo transport and protein turnover.<sup>2–4</sup> The 26S proteasome is an ATP-dependent protein degradation machine in the AAA+ (ATPases associated with diverse cellular activities) family of ATPases.<sup>5</sup> The proteasome holoenzyme consists of a barrel-shaped 20S core particle (CP) capped by 19S regulatory particles (RP) on one or both ends.<sup>6</sup> Each RP features a nine-member Lid subcomplex and a heterohexameric ring of AAA+ ATPases assembled from six distinct gene products.

The activities of proteasome are broadly driven by its structural dynamics which remains largely elusive. This has significantly limited our ability to understand the molecular basis for proteasome's functions and to interpret the experimental observations that are seemingly uncorrelated.<sup>1</sup> The exquisite dynamics of a large ATPase machine, such as the one on proteasome, remains difficult to probe experimentally. The ability to computationally simulate the proteasome system is limited both by its size and by the biological time scale. Though coarse-grained modeling and enhanced sampling schemes have been applied to study specific conformational steps of some ATPase systems,<sup>7–9</sup> an open-ended simulation of global ATPase dynamics, which is necessary for connecting with the rich biological activities of the proteasome, has not been reported. Special-purpose supercomputers, such as Anton, can achieve  $\sim 100 \mu\text{s/day}$  for a system of a similar size to the proteasome.<sup>10</sup> However, simulating such a system over a biologically relevant time scale (at least 100 ms for the proteasome) remains impractical for most researchers.

Here, we introduce a novel approach to obtain the empirical free-energy landscape (FEL) of the proteasomal ATPase complex and use the FEL to simulate the conformational dynamics of the ATPase



complex. We will elucidate the experimental and computational methods required for achieving these goals. As described in our original study, the simulation results are widely consistent with the experimental observations, such as rates of substrate and ATP hydrolysis, proteasome conformational occupancy and effects of proteasome mutations, both in our study and in previous literatures. This supports the validity of the FEL approach. We will provide various examples of using the FEL-based simulation to obtain mechanistic insights into the ATPase system.

Our study demonstrated the feasibility of simulating a complex protein machine such as the 26S proteasome. Our simulation results provided a coherent explanation for variety of structural and functional observations and revealed how the nonequilibrium dynamics of the AAA+ hexamer on the proteasome drove substrate translocation and led to various phenotypes in previous studies. The FEL approach represents an adaptable framework that can incorporate additional experimental knowledge to account for the ATPase dynamics more accurately for broader applications.

The workflow described in this protocol includes both experimental and computational methods, with the goal to guide the application and adaptation of the FEL approach. For the experimental part, standard lab practices should be followed for preparing buffers and media, and for protein purification. The guidelines by the original providers should be followed for culturing cell lines. Cell lines and the plasmids are available upon request. The software requires MATLAB environment which needs to be installed. The source code is available from Github.

Nomenclature:

- *State of the proteasome (or its ATPase complex)*: A combination of the conformation of the proteasome and its nucleotide distribution.
- *Free-energy landscape*: The standard free energy of a proteasome particle, as a function of its conformation and its nucleotide distribution; also referred to as the free-energy surface, energy surface or, more precisely, the potential of mean force.
- *Free-energy landscape model*: A mathematical model for the dynamics of the ATPase complex based on its free-energy landscape.
- *Dynamical space*: A representation of all possible states of the proteasome with the (usually steady-state) occupancy of the proteasome in each state and the transition rate between states.

## Buffer and reagents preparation

⌚ Timing: 1 day

1. Prepare buffers according to the instructions and recipes in [materials and equipment](#).
  - a. Buffers for protein purification: PBS, buffer P1 - 14.
  - b. Buffers and solutions for single-molecule fluorescence microscopy: TBS, UBAB, T50, W1, W2, PCA/PCD oxygen scavenging system.
  - c. Buffers and solutions for the 26S proteasome activity assay: W3, 50× ATP-regenerating system (E-mix).

## Protein purification

⌚ Timing: 2–3 weeks

This part describes the procedures for purifying all proteins required in the experiments in [step-by-step method details](#).

2. Purify the recombinant human N-terminal (1–88) cyclinB1 tagged with iRFP (cycB\_NT-iRFP) from NiCo21 DE3 cells using a polyHis-tag on the protein:

- a. Induce protein expression in DE3 cells transformed with the plasmid pT7-cycB\_NT-iRFP.
  - b. Lyse cells and bind proteins to the His60 Ni Superflow Resin in buffer P1.
  - c. Wash the resin once by buffer P1 and three times by buffer P2.
  - d. Elute proteins with buffer P3.
3. Biotinylate anti-20S antibody (MCP21) and bovine serum albumin (BSA) using biotin-NHS in PBS according to the manufacturers' instructions and purify them using Zeba desalting column. Store proteins in PBS.
  4. Purify recombinant Anaphase-promoting complex/cyclosome (APC)-Cdh1 from insect cells as described elsewhere.<sup>11–13</sup> Basic steps include:
    - a. Generate baculovirus expressing 14 APC components by transfecting Sf9 insect cells with the recombinant baculoviral genome based on a biGbac system using Cellfectin™ II Reagent.
    - b. Add amplified viruses to HighFive insect cell culture to express APC for 2–3 days.
    - c. Purify recombinant APC from cell lysate using Strep-Tactin sepharose based on a Twin-Strep(II)-tag on the C-terminus of APC4.

**Note:** The lysis buffer, wash buffer and elution buffer are listed as P4–P6.

- d. Concentrate the eluted proteins using 10 kD or 30 kD Amicon centrifugal filter.
- e. Add acTEV protease to the protein solution to cleave off the Strep-tag according to the manufacturer's instructions.
- f. Polish the protein by Mono Q 4.6/100 PE anion exchange chromatography.
  - i. Dilute protein sample into the same volume of buffer P7 without any salt.
  - ii. Filter the sample using 0.45 µm filter.
  - iii. Equilibrate the column and load the filtered sample.
  - iv. Run gradient of elution buffers from P7 to 60% P8. The APC should be eluted at 350–450 mM NaCl.
  - v. Collect and concentrate the fractions.
  - vi. Use the same concentrator to change the protein sample into buffer P9 by two times.
- g. Purify the co-activator Cdh1 with a N-terminal 3Myc-His6 tag from HighFive cells using Ni<sup>2+</sup> agarose.
  - i. Lyse cells and bind proteins to the His60 Ni Superflow Resin in buffer P10.
  - ii. Wash the resin with buffer P11.
  - iii. Elute proteins with buffer P12.
  - iv. Cleave off the 3Myc-His6 tag using thrombin protease for slightly higher activity.
5. Purify human 26S proteasome from a stable HEK293 cell line harboring HTBH-tagged hRPN11 (HEK293-Rpn11-HTBH). A detailed purification procedure can be found in Wang et al.<sup>14</sup>
  - a. Expand cells in 30 150 mm plates to full confluency and harvest.

**Note:** This may give you approximately 15–16 mL of cell pellet.

- b. Dounce-homogenize cells in the lysis buffer P13.
- c. Incubate the cleared lysate with NeutrAvidin agarose beads 12–16 h at 4°C.
- d. Wash the beads with excess lysis buffer followed by a wash buffer P14.
- e. Elute 26S proteasomes from the beads by cleavage using TEV protease in the same buffer P14 at 30°C for 2 h.

**Note:** There is no step for removing the TEV protease because the added TEV amount is insignificant and does not interfere with the downstream applications in our practice. In case that TEV needs to be removed, standard size-exclusion chromatography can be used.

- f. Collect the eluent and additionally about 3–4 more fractions by adding buffer P14.

- g. Concentrate the combined fractions using an Amicon centrifugal filter. An optional size-exclusion chromatography step (Superose 6) can be added to polish the proteasome sample.
- h. Run native PAGE and use the 26S proteasome activity assay (in the section of [the 26S proteasome activity assay](#)) to check the purity and activity of purified proteasomes.
- i. For purifying SNAP-tagged proteasome, the HTBH-Rpn11 cell line was stably transfected with a lentivirus carrying FLAG-SNAP-Rpn3 under a CMV promoter (HEK293-SNAP-Rpn3), and the SNAP proteasome can be purified from the transfected cell line using the above procedure.

**Note:** All protein samples are concentrated by Amicon centrifugal filter and concentrations are determined by Bio-Rad protein assay unless stated otherwise; Samples are snap-frozen and stored at  $-80^{\circ}\text{C}$  with 5%–10% (v/v) glycerol in the stock solution.

### Install software and download the source code

⌚ Timing: 1 day

This section describes the minimal hardware requirements, the installation procedures, as well as the source code. The recommended system configuration is a multi-core CPU of at least 2.5 GHz, at least 32 GB memory, Windows 7 or newer (macOS 10.11 or newer), MATLAB with toolboxes ver. 2016 or newer.

6. Download MATLAB with toolboxes and install.
7. Download the proteasome FEL model algorithm from the online deposit (<https://github.com/luyinghms/Proteasome-FEL-model.git>).
8. Add the algorithm folder to the MATLAB path following the online instructions on setting up MATLAB path: *MathWorks: Change Folders on Search Path* ([https://www.mathworks.com/help/matlab/matlab\\_env/add-remove-or-reorder-folders-on-the-search-path.html](https://www.mathworks.com/help/matlab/matlab_env/add-remove-or-reorder-folders-on-the-search-path.html)).
9. Download Pymol.
10. Download the proteasome structure analysis package from the online deposit (<https://github.com/fang688/Proteasome-structure-analysis>). The package contains:
  - a. The Pymol scripts of Cryo-EM structure analysis.
  - b. The PDB files of the 26S structure from the RCSB Protein Data Bank.<sup>15</sup>
  - c. Folders for separately saved ATPase interfaces and nucleotide-binding pockets coordinate files. More details are in step 1 of [step-by-step method details](#).
11. Add the structure analysis package to the working directory of the Pymol in the command window:

```
PyMOL> cd Path_of_the_structure_package
```

### KEY RESOURCES TABLE

REAGENT or RESOURCE	SOURCE	IDENTIFIER
<b>Antibodies</b>		
MCP21	Enzo Life Sciences	Cat. # BML-PW8105

(Continued on next page)

## Continued

REAGENT or RESOURCE	SOURCE	IDENTIFIER
<b>Bacterial and virus strains</b>		
NiCo21 DE3 (bacteria)	New England Biolabs	Cat. # C2529H
Recombinant baculoviral genome of Myc-6×His-Cdh1 (pFastBac system)	Brown et al. <sup>13</sup>	Myc-6×His-Cdh1
Recombinant baculoviral genome of Twin-Step(II)-APC (biGBac system)	Weissmann et al. <sup>11</sup>	Twin-Step(II)-APC
<b>Chemicals, peptides, and recombinant proteins</b>		
Alexa647-ATP	Invitrogen	Cat. # A22362
ATP-γS	Sigma-Aldrich	Cat. # A1388
Avidin-rhodamine red	Invitrogen	Cat. # A6378
Benzamidine hydrochloride hydrate	Sigma-Aldrich	Cat. # B6506
Benzonase nuclease	Millipore	Cat. # E1014
Biotin-NHS	Thermo Scientific	Cat. # 20217
Bovine serum albumin (BSA)	Cytiva	Cat. # SH30574
d-Desthiobiotin	Sigma-Aldrich	Cat. # D1411
Dichlorodimethylsilane (DDS)	Sigma-Aldrich	Cat. # 440272
EDTA-free protease inhibitor cocktail tablet	Roche	Cat. # 11873580001
Gamma-globulin	Sigma-Aldrich	Cat. # 345886
Human His6-ubiquitin E1 enzyme	R&D Systems	Cat. # E-304
Human ubiquitin	R&D Systems	Cat. # U-100H
Human His6-UbcH10/UBE2C	R&D Systems	Cat. # E2-650
Isopropyl-beta-D-thiogalactoside (IPTG)	Gold Biotechnology	Cat. # I2481C50
Pure ethanol	Decon Labs	Cat. # V1001
Pure hexane	Fisher Scientific	Cat. # H302
SNAP-surface 549	NEB	Cat. # S9112S
Streptavidin	Invitrogen	Cat. # 434302
Tween-20	Sigma-Aldrich	Cat. # P1379
TEV protease	Invitrogen	Cat. # 12575015
<b>Critical commercial assays</b>		
Bradford protein assay	Bio-Rad	Cat. # 5000205
Cellfectin™ II Reagent	Gibco	Cat. # 10362100
<b>Experimental models: Cell lines</b>		
HEK293	ATCC	CRL-1573
HEK293-Rpn11-HTBH	Wang et al. <sup>14</sup>	HEK293-Rpn11-HTBH
HEK293-Rpn11-HTBH cells with pCMV-FLAG-SNAP-Rpn3	Fang et al. <sup>1</sup>	HEK293-SNAP-Rpn3
HEK293-Rpn11-HTBH cells with pCMV-β1-FLAG-SNAP	Fang et al. <sup>1</sup>	HEK293-β1-SNAP
HighFive insect cells	Expression Systems	Cat. # 94-002F
Sf9 insect cells	Expression Systems	Cat. # 94-001F
<b>Recombinant DNA</b>		
pT7-cycB_NT-iRFP (plasmid)	Fang et al. <sup>1</sup>	pT7-cycB_NT-iRFP
pT7-human Ub (plasmid)	Fang et al. <sup>1</sup>	pT7-human Ub
<b>Software and algorithms</b>		
MATLAB 2018a	MathWorks	<a href="https://www.mathworks.com/products/matlab.html">https://www.mathworks.com/products/matlab.html</a>
Pymol Version 2.5.2	Schrodinger	<a href="https://pymol.org/2/">https://pymol.org/2/</a>
Proteasome FEL model algorithm	Fang et al. <sup>1</sup>	<a href="https://github.com/luyinghms/Proteasome-FEL-model.git">https://github.com/luyinghms/Proteasome-FEL-model.git</a>
Proteasome structure analysis package	Fang et al. <sup>1</sup>	<a href="https://github.com/fang688/Proteasome-structure-analysis">https://github.com/fang688/Proteasome-structure-analysis</a>
<b>Other</b>		
7×™ laboratory detergents	MP Biomedicals	Cat. # 97667095
1 mL syringe with attached needle 27 G × 1/2 in	BD	Cat. # 309623
10 kDa or 30 kDa Amicon centrifugal filter	Millipore	Cat. # UFC5010, UFC5030, UFC8010, UFC8030
150 mm TC-treated cell culture dish	Falcon	Cat. # 353025

(Continued on next page)

**Continued**

REAGENT or RESOURCE	SOURCE	IDENTIFIER
384-wells plate	Corning	Cat. # 4514
5-slide mailer - open top	Electron Microscopy Sciences	Cat. # 71548
50 × 24 mm No. 1 glass coverslips	VistaVision, VWR	Cat. # 16004-098
Antibiotic antimycotic solution (100×)	Sigma-Aldrich	Cat. # A5955
Coverglass staining rack	Electron Microscopy Sciences	Cat. # 72239-04
Digital pro ultrasonic cleaner	VEVOR	Model 10L/2.5 Gal
Digital sonifier	VWR	Branson Sonifier 450
DMEM	Wisent Bioproducts	Cat. # 319-015-CL
Dynabeads™ His-Tag beads	Invitrogen	Cat. # 10103D
ESF 921 medium	Expression Systems	Cat. #96-001-01
Fetal bovine serum (FBS)	Gibco	Cat. # 10438026
His60 Ni superflow resin	Takara Bio	Cat. # 635660
Microplate reader with an infrared filter (EX 640/40; EM 720/10)	BioTek	Synergy H1
Milli-Q water	EMD Millipore	Millipak® Express 40 Filter
Mono Q 4.6/100 PE	Sigma-Aldrich	Cat. # GE17-5179-01
NeutrAvidin agarose	Thermo Scientific	Cat. # 29200
Protein LoBind tubes	Eppendorf	Cat. # 0030108434, 0030108442
Rocker shaker	Scientific Industries	Model # SI-110
Strep-Tactin sepharose	iba	Cat. # 2-1201
Syringe filter unit, 0.45 µm, PVDF	Millipore	Cat. # SLHVM33RS
TIRF microscope with three laser lines of 488 nM (150 mW), 561 nM (150 mW), 638 nM (100 mW), and a Pco sCMOS camera	Customized	N/A
Vacuum seal machine and bags	Foodsaver	Model # FSFSBF0226-FFP
Zeba desalting column	Thermo Scientific	Cat. # 89877, 89882
Compressed air	N/A	N/A
Flame	N/A	N/A
Nitrogen gas	N/A	N/A

## MATERIALS AND EQUIPMENT

**Note:** The pH of all buffers is measured at 25°C.

**Note:** Buffers and solutions are prepared in ddH<sub>2</sub>O unless stated otherwise.

### Common buffers

PBS (pH 7.4)	
Reagent	Final concentration
Na <sub>2</sub> HPO <sub>4</sub>	10 mM
KH <sub>2</sub> PO <sub>4</sub>	1.8 mM
NaCl	137 mM
KCl	2.7 mM
ddH <sub>2</sub> O	N/A

**Note:** PBS can be stored at 25°C for 1 year.

- TBS: 50 mM Tris-HCl pH 7.5, 150 mM NaCl in ddH<sub>2</sub>O.

**Note:** TBS can be stored at 25°C for 1 year.

- UBAB: 25 mM Tris-HCl pH 7.5, 50 mM NaCl, 10 mM MgCl<sub>2</sub> in ddH<sub>2</sub>O.

**Note:** UBAB can be stored at 25°C for 1 year.

- T50: 20 mM Tris-HCl pH 8.0, 50 mM NaCl in ddH<sub>2</sub>O.

**Note:** T50 can be stored at 25°C for 1 year.

## Buffers for protein purification

<b>P1</b>	
Reagent	Final concentration
Tris-HCl pH 7.5	30 mM
NaCl	300 mM
MgCl <sub>2</sub>	5 mM
PMSF	1 mM
Glycerol	10% (v/v)
Tween-20	0.5% (v/v)
Imidazole	10 mM
ddH <sub>2</sub> O	N/A

**Note:** Buffer P1 needs to be freshly prepared and stored at 4°C.

<b>P2</b>	
Reagent	Final concentration
Tris-HCl pH 7.5	30 mM
NaCl	300 mM
MgCl <sub>2</sub>	5 mM
PMSF	0.1 mM
Glycerol	10% (v/v)
Tween-20	0.05% (v/v)
Imidazole	10 mM
ddH <sub>2</sub> O	N/A

**Note:** Buffer P2 needs to be freshly prepared and stored at 4°C.

<b>P5</b>	
Reagent	Final concentration
Tris-HCl pH 8.3	50 mM
NaCl	200 mM
Glycerol	5% (v/v)
DTT	2 mM
EDTA	1 mM
Benzamidine	0.33 mg/mL
ddH <sub>2</sub> O	N/A

**Note:** Buffer P5 needs to be freshly prepared and stored at 4°C.

<b>P7</b>	
Reagent	Final concentration
Hepes pH 8.0	20 mM
NaCl	50 mM

(Continued on next page)



**Continued**

Reagent	Final concentration
Glycerol	5% (v/v)
DTT	2 mM
EDTA	1 mM
ddH <sub>2</sub> O	N/A

**Note:** Buffer P7 needs to be freshly prepared and stored at 4°C.

**P8**

Reagent	Final concentration
Hepes pH 8.0	20 mM
NaCl	1 M
Glycerol	5% (v/v)
DTT	2 mM
EDTA	1 mM
ddH <sub>2</sub> O	N/A

**Note:** Buffer P8 needs to be freshly prepared and stored at 4°C.

**P9**

Reagent	Final concentration
Hepes pH 8.0	20 mM
NaCl	150 mM
Glycerol	5% (v/v)
DTT	1 mM
ddH <sub>2</sub> O	N/A

**Note:** Buffer P9 needs to be freshly prepared and stored at 4°C.

**P10**

Reagent	Final concentration
Hepes pH 7.0	20 mM
(NH <sub>4</sub> ) <sub>2</sub> SO <sub>4</sub>	100 mM
Glycerol	5% (v/v)
DTT	1 mM
Imidazole	20 mM
EDTA-free protease inhibitor cocktail	1 ×
ddH <sub>2</sub> O	N/A

**Note:** Buffer P10 needs to be freshly prepared and stored at 4°C.

**P11**

Reagent	Final concentration
Hepes pH 7.0	20 mM
(NH <sub>4</sub> ) <sub>2</sub> SO <sub>4</sub>	300 mM
Glycerol	2.5% (v/v)
DTT	1 mM
Imidazole	20 mM
ddH <sub>2</sub> O	N/A

**Note:** Buffer P11 needs to be freshly prepared and stored at 4°C.

P13	
Reagent	Final concentration
NaH <sub>2</sub> PO <sub>4</sub> pH 7.5	50 mM
NaCl	100 mM
Glycerol	10% (v/v)
DTT	1 mM
NP-40	0.5% (v/v)
ATP	5 mM
MgCl <sub>2</sub>	5 mM
EDTA-free protease inhibitor cocktail	1 ×
Phosphatase inhibitor	1 ×
ddH <sub>2</sub> O	N/A

**Note:** Buffer P13 needs to be freshly prepared and stored at 4°C.

- P3: Add 250 mM imidazole to P2.

**Note:** Buffer P3 needs to be freshly prepared and stored at 4°C.

- P4: Add 0.1 mM PMSF, 1 × EDTA-free protease inhibitor cocktail, 5 u/mL benzonase to P5.

**Note:** Buffer P4 needs to be freshly prepared and stored at 4°C.

- P6: Add 2.5 mM desthiobiotin to P5.

**Note:** Buffer P6 needs to be freshly prepared and stored at 4°C.

- P12: Add 250 mM imidazole to P11.

**Note:** Buffer P12 needs to be freshly prepared and stored at 4°C.

- P14: 50 mM Tris-HCl pH 7.5, 10% (v/v) glycerol, 1 mM ATP-MgCl<sub>2</sub> in ddH<sub>2</sub>O.

**Note:** Buffer P14 needs to be freshly prepared and stored at 4°C.

△ **CRITICAL:** Chemicals including ATP, DTT, PMSF, protease inhibitor and phosphatase inhibitor need to be freshly added to the buffer after which the buffer needs to be always kept on ice or at 4°C.

## Other buffers and solutions

PCA	
Reagent	Final concentration
Protocatechuic acid (PCA)	100 mM
NaOH	adjust pH to 9.0
ddH <sub>2</sub> O	N/A

**Note:** PCA solution can be stored at  $-80^{\circ}\text{C}$  for 1 year.

<b>PCD</b>	
Reagent	Final concentration
Protocatechuate-3,4-dioxygenase (PCD)	10 mg/mL
Tris-HCl pH 8.0	100 mM
KCl	50 mM
Glycerol	50% (v/v)
EDTA	1 mM
ddH <sub>2</sub> O	N/A

**Note:** PCD solution can be stored at  $-80^{\circ}\text{C}$  for 1 year.

- W1: 0.05% (v/v) Tween-20, 0.5 mM DTT in 1× UBAB.

**Note:** Buffer W1 can be stored at  $-20^{\circ}\text{C}$  for 1 month.

- W2: 0.005% (v/v) Tween-20, 0.5 mM DTT in 1× UBAB.

**Note:** Buffer W2 can be stored at  $-20^{\circ}\text{C}$  for 1 month.

- W3: 0.05% (v/v) NP-40, 1 mM DTT, 0.5 mg/mL gamma-globulin, 10% glycerol (v/v) in 1× UBAB.

**Note:** Buffer W3 can be stored at  $-20^{\circ}\text{C}$  for 1 month.

- 50× ATP-regenerating system (E-mix): 1 M phosphocreatine, 5 mg/mL creatine kinase, 50 mM ATP in 50× UBAB.

**Note:** 50× E-mix can be stored at  $-20^{\circ}\text{C}$  for 1 month.

## STEP-BY-STEP METHOD DETAILS

Here, we will describe how to determine the FEL of the proteasomal ATPase complex and use it to study the ATPase dynamics. We will first cover the steps for the FEL model construction and explain the details on determining the model parameters using the single-molecule proteasome-nucleotide interaction assay and the 26S proteasome activity assay. We will then explain how to simulate the dynamics of the ATPase complex based on its FEL and provide examples for how to obtain mechanistic insights from the simulation results.

### FEL model construction

⌚ Timing: 1 week

In this section, we will explain how to construct a nucleotide-dependent FEL of the ATPase complex on the 26S proteasome. The procedure has three steps: 1. Defining proteasome's conformational space based on its cryo-EM structures; 2. Parameterizing the free energy as a function of the ATPase conformation and the nucleotide distribution; 3. Experimentally determining the model parameters.

1. Analyze cryo-EM structures of the proteasome.
  - a. Launch Pymol.

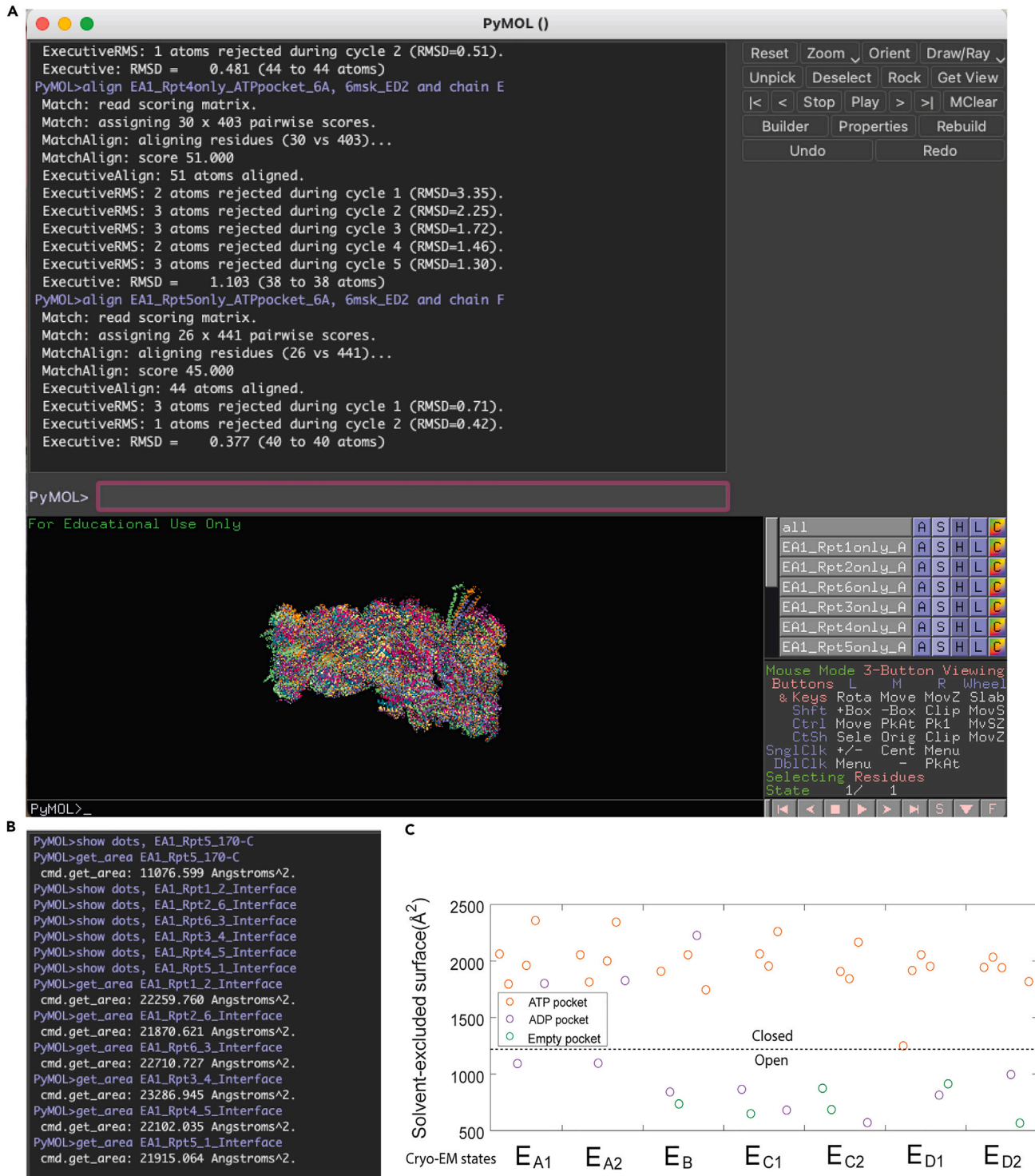


**Figure 1. Analysis of proteasome's cryo-EM structures**

(A) Pymol interface after running the script *Pymol\_script2\_RMSD.txt* to align nucleotide-binding pockets of the proteasome and calculate the root-mean-square-deviation (RMSD) of the aligned *cis* elements of the nucleotide pocket. The RMSDs are reported in the command window (upper left); The aligned structures are shown in the display window (lower left).

(B) The command window displaying the solvent-accessible surface area (SASA) calculated by running the script *Pymol\_script3\_SASA.txt*.

(C) The solvent-excluded surface area (SESA) at the interfaces of the ATPase domains in the seven substrate-engaged proteasome structures, colored according to the nucleotide at each binding pocket. The dashed line separates the closed and open interfaces. Reproduced from Fang et al.<sup>1</sup> No permission is required.

- b. Define the nucleotide-binding pocket of each ATPase subunit (Rpt1~6) based on the structure of E<sub>A1</sub> state by selecting amino acids within 6–9 Å of the bound nucleotide.

**Note:** The Pymol script is available as Pymol\_script1\_DefineATPpocket.txt. The PDB files of the identified pockets are saved in the folder ATPpocket.

- c. Calculate the root-mean-square-deviation (RMSD) of the nucleotide pocket.
  - i. Align structures of each nucleotide-binding pocket in different states of the proteasome.
  - ii. Calculate the RMSD of the aligned atoms of the *cis* elements of the nucleotide pocket.

**Note:** The Pymol script is available as Pymol\_script2\_RMSD.txt. The RMSD is reported in the command window (Figure 1A).

**Note:** The observation that the *cis* elements of the nucleotide-binding pockets exhibit rather minor rearrangements among different structures ([RMSD] ~ 0.58 Å) is the basis for step 4, which was discussed in details in Fang et al.<sup>1</sup>

- d. Calculate the solvent-accessible surface area (SASA) for each pair of two adjacent ATPase domains in isolation (SASA<sub>ATPase1</sub>, SASA<sub>ATPase2</sub>) and in the complex (SASA<sub>ATPase1-ATPase2</sub>).

**Note:** The Pymol script is available as Pymol\_script3\_SASA.txt. The PDB files of each ATPase pair are saved in the folder ATPinterface. The surface area is reported in the command window (Figure 1B).

- e. Calculate the solvent-excluded surface area (SESA) formed by the interacting residues using the formula:

$$\text{SESA}_{\text{ATPase1-ATPase2}} = [\text{SASA}_{\text{ATPase1}} + \text{SASA}_{\text{ATPase2}} - \text{SASA}_{\text{ATPase1-ATPase2}}] / 2.$$

**Note:** The observation that the SESAs of the ATPase interfaces mostly adopt binary values in the cryo-EM structures is the basis for step 2 (Figure 1C).

2. Define the conformational space in the FEL model.
  - a. Define each conformation in the FEL by the status of the six ATPase domain interfaces, being either open (small SESA) or closed (large SESA).

**Note:** The total number of open interfaces in each conformation is constrained to be either 2 or 3, since only 2 or 3 open interfaces have been observed in the cryo-EM structures of the proteasome. Five conformations having 3 + 3 or 2 + 2+2 symmetry in the ATPase architecture are excluded to avoid ambiguity in assigning substrate-ATPase interaction. The FEL totally contains 30 discrete conformations (Table 1).

- b. Define each state in the FEL model as a unique combination of an ATPase conformation and a nucleotide distribution in the six binding pockets.

**Note:** In our practice, each nucleotide pocket can be empty, ATP-bound, ADP-bound, or ATP-γS-bound. The total number of states in the nucleotide-dependent FEL is  $30 \times 4^6 = 122880$ .

**Note:** "Interface": the 6 digits indicate the status of Rpt6-Rpt3, Rpt3-Rpt4, Rpt4-Rpt5, Rpt5-Rpt1, Rpt1-Rpt2, Rpt2-Rpt6 interfaces: "0" means open interface; "1" means closed interface.

**Table 1. ATPase conformations**

Index	Interface	Engagement	Index	Interface	Engagement
1	000111	100111	16	100110	000111
2	001011	100011	17	100111	110111
3	001101	001110	18	101001	110001
4	001110	001111	19	101011	110011
5	001111	101111	20	101100	001110
6	010011	100011	21	101110	001111
7	010110	000111	22	110001	111001
8	010111	100111	23	110010	111000
9	011001	011100	24	110011	111011
10	011010	011100	25	110100	111000
11	011100	011110	26	110101	111001
12	011101	011110	27	111000	111100
13	011110	011111	28	111001	111101
14	100011	110011	29	111010	111100
15	100101	110001	30	111100	111110

"Engagement": the 6 digits indicate the substrate engagement status of Rpt6, Rpt3, Rpt4, Rpt5, Rpt1, Rpt2 subunits: "0" means disengaged subunit; "1" means engaged subunit.

### 3. Collect the empirical rules for FEL model construction based on cryo-EM observations.

**Note:** There is no gold standard for generalizing the observations as rules in the model. More rules than necessary might be collected at the beginning. The importance of each rule needs to be assessed later by the model to generate a minimal set of rules that still allow accurate prediction of proteasome's behaviors. Here we list the important rules we found.

- A series of closed interfaces arrange the substrate-interacting motif pore-1 loop (PL1) of consecutive ATPases into a staircase architecture. Those ATPases are defined as "engaged" subunits with 2-amino acid (AAs) axial separation between their PL1s (Table 1).
- One or a stretch of ATPase subunits that are flanked by open interfaces on both sides are disengaged from substrate interaction, and their PL1s move to the top registry of the staircase.
- Each state of the ATPase complex contains at least one disengaged subunit.

**Note:** In the scenarios involving three ATPase segments, the largest segment is assumed to interact with the substrate.

- During each step of conformational transition, the substrate translocation distance is taken as the difference between the average staircase positions of those engaged ATPases before and after the transition.
- ### 4. Parameterize the free-energy function.

The free energy of each state is expressed as the sum of the contributions from each individual ATPase interface that depends on the following key parameters:

- The nucleotide binding rate  $k_{on}$ , binding energy of nucleotide to the *cis* pocket of the engaged subunit  $e_p$ , binding energy of the nucleotide to the *cis* pocket of the disengaged subunit  $e_p^{APO}$ , basal energy of nucleotide-independent interaction between adjacent ATPases  $e_B$  are all inferred from published results.<sup>15–20</sup>
- The nucleotide unbinding rate  $k_{off}$  is calculated based on the formula:

$$k_{off} = k_{on} \cdot e^{\frac{(e_p + e_B + e_p^{APO})}{kT}} \cdot C_0,$$

where  $e_{Br}$  is the bridge energy described below;  $C_0$  is the standard concentration 1 M.

- c. The difference of the bridge energy ( $e_{Br}^{ADP} - e_{Br}^{ATP}$ ) that differentiate ADP from ATP in interacting with the *trans* ATPase is determined by a quantitative assay described in the following section of [single-molecule proteasome-nucleotide interaction assay](#). The absolute values of  $e_{Br}^{ADP}$ ,  $e_{Br}^{ATP}$  are then inferred from published results.<sup>21</sup>

**Note:** This energy difference is the key for directional translocation of substrate by the ATPase machine.

**Note:** The detailed calculation has been explained in Fang et al.<sup>1</sup>

5. Determine the kinetic parameters related to substrate translocation.

- a. Calculate the transition rate  $r_{AB}$  from conformation A to B by the following Arrhenius equation:

$$r_{AB} = k_0 \cdot e^{(E(A) - E(B) - f_{AB} \cdot d_{AB})/2kT},$$

where  $E(A)$ ,  $E(B)$  are standard free energy of the conformational state A and B at a given nucleotide status;  $f_{AB}$  is the average force on substrate during the translocation with two different values for the forward and the backward translocation to reflect the dissipative and conservative parts of this force;  $d_{AB}$  is the translocation distance associated with the conformational change from A to B;  $k_0$  is a constant pertaining to the activation energy barrier. The factor '2' comes from detailed balance.  $f_{AB}$  and  $k_0$  are determined by the quantitative assay described in the section of [the 26S proteasome activity assay](#).

**Note:** The substrate peptide is assumed to be tightly gripped by the PL1 on the ATPases without slippage during translocation.

- b. The ATP hydrolysis rate  $k_h$  of each pocket is chosen to make the ATP consumption rate in the simulation of the FEL model match the experimental values, which will be further discussed in the section of *Monte Carlo simulation of ATPase dynamics using the FEL model*.

**Note:** We assign the same set of energy and kinetic parameters to the six ATPases on the proteasome, except for the basal energy  $e_B$  whose values are randomly drawn from a uniform distribution with zero mean and a small magnitude of 0.2 kcal/mol for each interface in each simulation to circumvent the ambiguity due to energy level degeneracy. All parameters in the FEL model are summarized in [Table 2](#) and [Figure 2](#).

## Single-molecule proteasome-nucleotide interaction assay

⌚ Timing: 3 days

In this section, we detail how to determine the energy parameters based on the affinities of different nucleotides to the ATPase pockets, as measured using single-molecule Total Internal Reflection Fluorescence (TIRF) microscopy ([Figure 3A](#)).

6. Perform coverslip cleaning and salinization.

- a. Clean the standard 50 × 24 mm No. 1 glass coverslips thoroughly by 7× Laboratory Detergent, pure ethanol, 1 M KOH and Milli-Q water by sonicating in the digital pro ultrasonic cleaner following the procedures described in Hon et al.<sup>23</sup>
- b. Dry the coverslips with a steady flow of compressed air after wash.
- c. Flame the dried coverslip for 3 s on both sides and allow it to cool in air.
- d. Rinse the coverslips once with pure hexane to remove residual water.

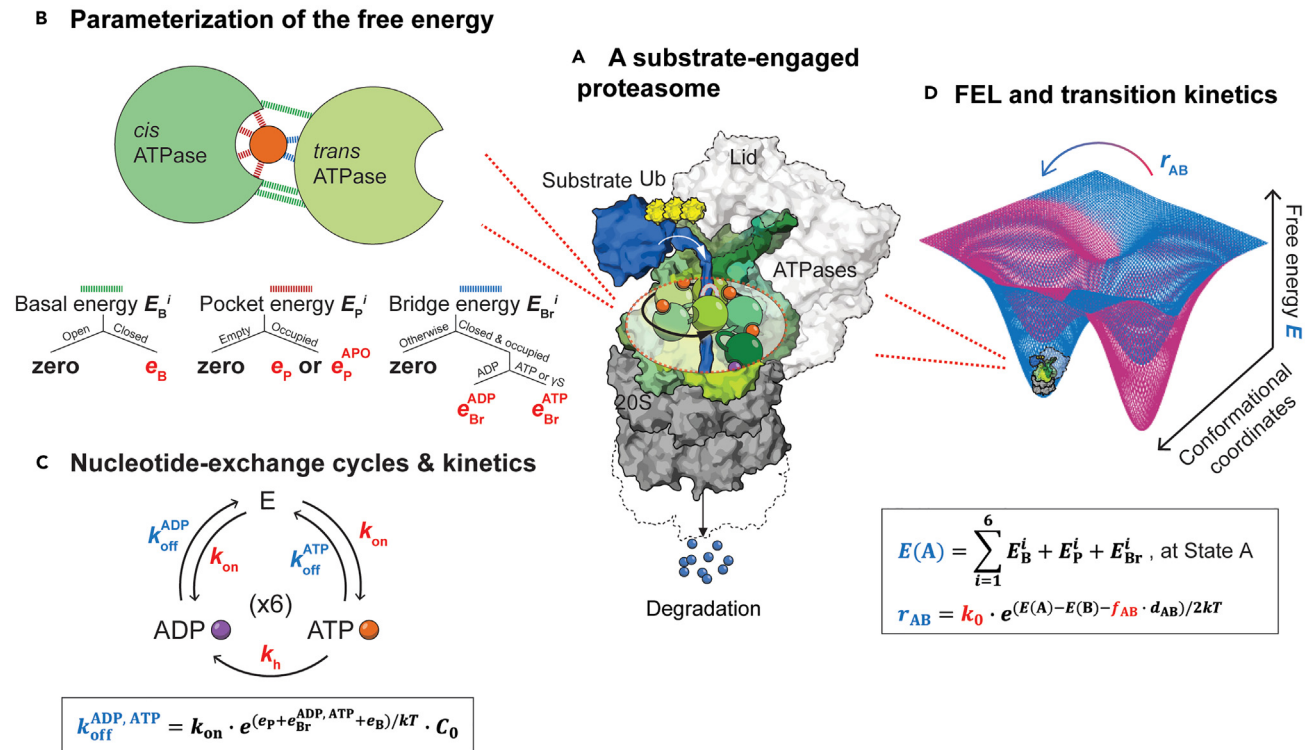


**Figure 2. Summary of all experimentally determined parameters (in red, as listed in Table 2) and variables (in blue, calculated according to the formulae in boxes) in the FEL model.**

(A) A schematic for a half 26S proteasome engaged with an unfolded substrate through the PL1s (color loops) on the ATPase subunits with bound nucleotides (color blobs), reproduced from Fang et al.<sup>1</sup> (B) The system's free energy is parameterized based on ATPase-nucleotide interactions at each binding pocket which can be subdivided into three terms: the basal energy  $E_B^i$ , the pocket energy  $E_P^i$  and the bridge energy  $E_{Br}^i$  ("i" indicates the i th ATPase). The total free energy is then calculated as a sum of the contributions from each individual pocket based on the formula in (C). (C) Nucleotide-exchange cycles at six pockets proceed independently ("x6" indicates 6 ATP cycles in total) with kinetic parameters  $k_{on}$ ,  $k_{off}$ , and  $k_h$ . (D) The FEL of the proteasome is altered by nucleotide exchange or reaction (two colors indicate different nucleotide-binding states), triggering the transitions between conformations. The transition kinetics is modeled as a simple bi-state process with a rate constant  $r_{AB}$  determined by the Arrhenius equation.

- e. Immerse cleaned coverslips in a solution of 0.25% (v/v) dichlorodimethylsilane (DDS) in pure hexane for 1.5 h on a rocker shaker. Sonicate the coverslips for 1 min in the middle of the reaction to remove attached bubbles.

**Note:** Use a syringe to take DDS from the bottle and inject below the surface of hexane. Don't take the DDS bottle out of the refrigerator to avoid condensation. Seal the bottle immediately after use.

- f. Rinse the coverslips twice with hexane, during the second time, sonicate for 1 min.
- g. Wash coverslips extensively with Milli-Q water by 3 times. During each wash, immerse the coverslips with Milli-Q water, shake for 30 s, and then dump all water completely.
- h. Separate surfaces and rinse in Milli-Q water.
- i. Dry the coverslips with a steady flow of nitrogen gas.
- j. Store the coverslips in open-top 5-slide mailers and vacuum-sealed bags at  $-20^{\circ}\text{C}$  for up to 12 months without loss of quality.

**Note:** Drill a hole in the cap of the slide mailer to guarantee vacuum inside. Each coverslip is put on the top of a clean slide inserted to the mailer. The surface not touching the slide is used for imaging.



**Table 2. Parameters in the FEL model**

Parameter	Description	Value	Source
$k_{on}$	nucleotide binding rate	1e5 /M/s	Al-Shawi et al. <sup>16</sup> ; Fang et al. <sup>1</sup>
$k_{off}$	nucleotide dissociation rate	$k_{on} e^{(e_p + e_{Br} + e_B)/kT}$	Fang et al. <sup>1</sup>
$e_B$	basal energy	0	*Not affecting results
$e_{Br}^{ADP}$	bridge energy for ADP	-0.52 kcal/mol	Fang et al. <sup>1</sup>
$e_{Br}^{ATP}$	bridge energy for ATP	-2.1 kcal/mol	Fang et al. <sup>1</sup>
$e_p$	pocket energy	-7.4 kcal/mol	Kim et al. <sup>19</sup> ; Majumder et al. <sup>18</sup>
$e_p^{APO}$	pocket energy of APO state	-3.7 kcal/mol	dela Pena et al. <sup>17</sup> ; Dong et al. <sup>15</sup> ; Eisele et al. <sup>20</sup>
$f_{AB}$ (forward)	average force on forward translocated substrate	1.8 pN	Fang et al. <sup>1</sup>
$f_{AB}$ (backward)	average force on backward translocated substrate	0.56 pN	Fang et al. <sup>1</sup>
$k_0$	constant related to energy barrier	72 /sec	Fang et al. <sup>1</sup>
$k_h$	ATP hydrolysis rate	1.4 /sec/subunit	Peth et al. <sup>22</sup> ; Fang et al. <sup>1</sup>

7. Assemble the flow chamber according to the detailed procedures described in Hon et al.<sup>23</sup> The final flow cell schema is shown in Figure 3B.

**Note:** Flow cells can be stored in vacuum-sealed bags at  $-20^{\circ}\text{C}$  until use.

8. Evaluate the quality of imaging surface.

Coverslips and flow cells are prepared for assays to measure the binding affinity of nucleotides to the proteasomal ATPases through monitoring the steady-state occupancy rate of the labeled proteasome by fluorescence-labeled nucleotides. To assess suitability of the imaging surface for the assays, the control experiments to determine the binding capacity of the biotin-tagged proteasome to the surface and the level of the nonspecific binding of the nucleotide to the surface are necessary.

- a. Inject 0.2 mg/mL biotinylated BSA in T50 buffer into the chamber and incubate for 5 min at  $20^{\circ}\text{C}$ – $25^{\circ}\text{C}$ .
- b. Rinse 3 times with 200  $\mu\text{L}$  buffer W1.
- c. Inject 0.2% (v/v) Tween-20 in buffer W1 into the chamber and incubate for 10 min at  $20^{\circ}\text{C}$ – $25^{\circ}\text{C}$ .
- d. Rinse 3 times with 200  $\mu\text{L}$  buffer W1.
- e. Inject 40 mg/mL gamma-globulin solution (dissolved in TBS) + 0.1% (v/v) Tween-20 into the chamber and incubate for 10 min at  $20^{\circ}\text{C}$ – $25^{\circ}\text{C}$ .
- f. Rinse 3 times with 200  $\mu\text{L}$  buffer W1.
- g. Inject the avidin-rhodamine red solution in buffer W1 with a known concentration into the chamber and incubate for 2 min.

**Note:** Any dye-conjugated avidin can be used here, as long as its spectrum does not overlap with that of Alexa647. A titration of various concentration is recommended. We usually start with 2 mg/mL avidin-dye stock solution and dilute it 10–50 folds in buffer W1.

- h. Wash the chamber with 200 nM Alexa647-ATP in buffer W1.
- i. Image immediately at both 561 nm and 640 nm channels using a customized TIRF microscope.

**Note:** Any commercial or customized TIRF microscope should work here.

- j. Check the density of the rhodamine on the surface to determine the concentration of streptavidin and proteasome to use for a good surface density.

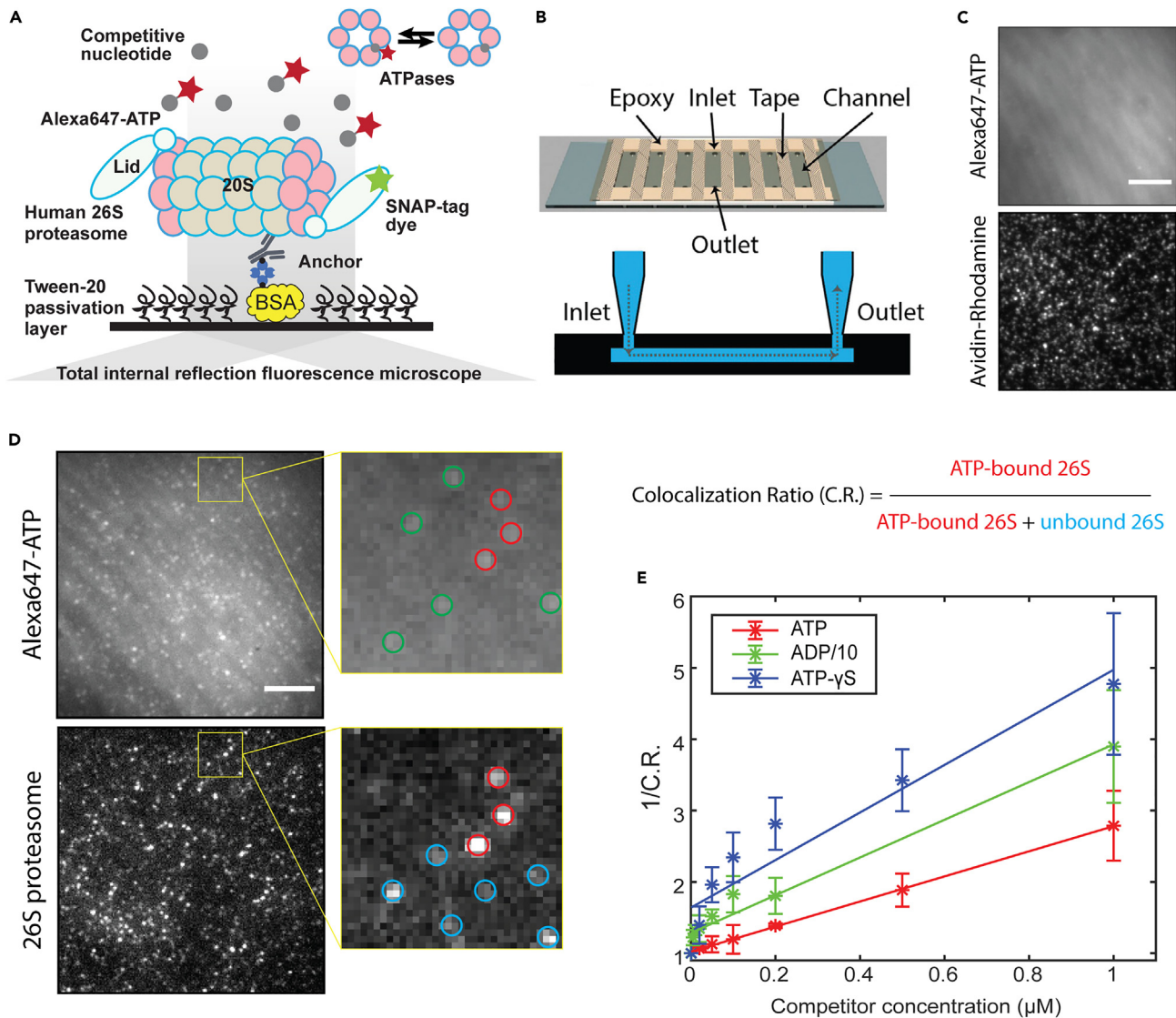


**Figure 3. Single-molecule proteasome-nucleotide interaction assay**

(A) Experimental setup of the single-molecule assay. Alexa647-ATP is mixed with the dark nucleotide (gray spheres) as a competitor, incubated with surface-immobilized 26S proteasome labeled with a SNAP-tag dye. The interaction of Alexa647-ATP with proteasome in a steady state is measured using a TIRF microscope.

(B) Flow cell schematic showing the components described in step 7. Reproduced from Hon et al.<sup>23</sup> Permission has been obtained.

(C) Example images of good surface density of avidins (40 μg/mL) and rare nonspecific binding of Alexa647-ATP. Scale bar: 10 μm.

(D) Single-particle identification of the Alexa647-ATP and the proteasome and calculation of their colocalization ratio (C.R.). C.R. is defined as the ratio of the number of proteasomes colocalized with Alexa647-ATP (red circle) and the total proteasome number (red and blue circles). The free Alexa647-ATP is circled in green. Scale bar: 10 μm.

(E) C.R. after normalization by the competitor-free condition was inversely regressed on the competitor concentration to obtain the relative inhibitor constant  $K_{nt}$  as described in step 12. ADP concentration is divided by 10 for presentation. Error bars represent the standard deviation of three experimental replicates. Reproduced from Fang et al.<sup>1</sup>

**Note:** The upper limit of the surface density of bound avidin is shown in Figure 3C. Higher density is not recommended which causes difficulty in single-particle identification.

- k. Count the number of Alexa647 molecules in the field of view. For a surface of good quality, we normally identify < 5 molecules of Alexa647-ATP in a 40 × 40 μm field of view (Figure 3C).

9. Prepare fluorescently labeled proteasome.
  - a. Incubate 30  $\mu$ L 50 nM purified SNAP-Rpn3 proteasome with 2 mg/mL BSA, 60 nM biotinylated MCP21 antibody and 1  $\mu$ M SNAP-surface 549 dye for 30 min at 20°C–25°C in the original storage buffer of the proteasome.
  - b. Change the buffer of the proteasome-antibody mix into buffer W2 + 0.4 mg/mL BSA using a 0.5 mL 30kD concentrator at 4°C; and then buffer exchange again into buffer W2 without BSA; finally change the buffer to W2 + 1  $\mu$ M Alexa647-ATP.

**Note:** This step is to remove the free MCP21 and the label-free ATP molecules from the proteasome stock solution.

- c. Dilute the proteasome solution by 5 folds in buffer W1 with various concentrations of competitive nucleotides ADP, ATP or ATP- $\gamma$ S, and 200 nM Alexa647-ATP.

**Note:** 2 mM protocatechuic acid (PCA), and 0.5 mg/mL protocatechuate-3,4-dioxygenase (PCD) are recommended here as the oxygen scavenging system and triplet state quencher to protect dye molecules from photobleaching.

- d. Incubate the proteasome sample for 20 min on ice.

**Note:** We did not observe obvious proteasomal 19S-20S dissociation as suggested by the stable fluorescent SNAP-Rpn3 signal during a 30-minute incubation inside the chamber monitored by the time-lapse imaging.

**Note:** For each concentration of the competitive nucleotides, prepare at least 3 replicates for imaging and quantification to reduce error.

10. Image the interaction of the 26S proteasome with Alexa647-ATP by TIRF microscopy ([Figure 3A](#)).
  - a. Assemble the image chamber and perform steps 8.a–f.
  - b. Dilute 5  $\mu$ L 20 mg/mL streptavidin solution (in TBS) to 70  $\mu$ L 40 mg/mL gamma-globulin solution (in TBS), mix well, and inject the solution into the flow cell channel, and incubate at 20°C–25°C for 1 min.
  - c. Rinse 3 times with 400  $\mu$ L buffer W1.
  - d. Load the proteasome solution from step 9 into the channel and incubate for 2 min.
  - e. Image the surface using the TIRF microscope. Acquire a short time-lapse at 200 ms frame-rate.

**Note:** A single snap-shot at both 561 nm and 640 nm channels is necessary for steady-state quantification. Here we acquire a short time-lapse mainly to reduce false positive rates in single-particle identification as we discard particles that appear only in one frame.

11. Measure the colocalization ratio of the Alexa647-ATP and the proteasome ([Figure 3D](#)).
  - a. Perform the basic image processing and the single-particle identification in both 561 nm and 640 nm channels as described in Hon et al.<sup>23</sup>
  - b. Perform colocalization analysis of the proteasome and Alexa647-ATP. Two molecules are marked as “colocalized” once the centers of mass of the identified proteasome and Alexa647-ATP from step 11.a have a distance within 1 pixel (0.26  $\mu$ m). Calculate the colocalization ratio C.R. as the fraction of SNAP-tagged proteasome particles that interact with Alexa647-ATP at steady-state.
  - c. For each type of the competitive nucleotide, vary its concentration [nt] to measure the corresponding C.R. value.

12. Perform linear regression of  $\frac{1}{\text{C.R.}}$  and  $[\text{nt}]$  to get the slope  $s_{\text{nt}} = \frac{K_{\text{ATP}^*}}{[\text{ATP}^*]K_{\text{nt}}}$  based on the following formula (Figure 3E):

$$\text{C.R.} = \frac{[\text{ATP}^*]}{K_{\text{ATP}^*} \left( 1 + \frac{[\text{nt}]}{K_{\text{nt}}} \right) + [\text{ATP}^*]},$$

$$1/\text{C.R.} = 1 + \frac{K_{\text{ATP}^*}}{[\text{ATP}^*]} + \frac{K_{\text{ATP}^*}}{[\text{ATP}^*]K_{\text{nt}}} [\text{nt}],$$

where  $[\text{ATP}^*]$  is the concentration of Alexa647-ATP;  $K_{\text{ATP}^*}$  is the dissociation constant of Alexa647-ATP;  $[\text{nt}]$  is the concentration of the competitive nucleotide;  $K_{\text{nt}}$  is the inhibitor constant of the competitive nucleotide.

13. Calculate the difference of the bridge energy of two types of nucleotides  $e_{\text{Br}}^{\text{nt1}} - e_{\text{Br}}^{\text{nt2}}$  based on the following formula:

$$e_{\text{Br}}^{\text{nt1}} - e_{\text{Br}}^{\text{nt2}} = kT \ln \left( \frac{K_{\text{nt1}}}{K_{\text{nt2}}} \right) = kT \ln \left( \frac{s_{\text{nt2}}}{s_{\text{nt1}}} \right)$$

where  $s_{\text{nt1}}$ ,  $s_{\text{nt2}}$  are the slopes fitted in step 12.

**Note:** We use a very low concentration of Alexa647-ATP in the assay (200 nM), which guarantees that the detection of the nucleotide binding event is restricted to the single ATPase pocket with the strongest binding affinity as discussed in Fang et al.<sup>1</sup>

**Note:** To minimize the effect of nucleotide hydrolysis, it is preferable to use the slowly-hydrolyzing ATP analog ATP- $\gamma$ S as the competitive nucleotide to measure the binding affinity of ATP.

## The 26S proteasome activity assay

⌚ Timing: 1 day

In this section, we describe a quantitative assay to determine the activity of the 26S proteasome under various conditions, based on the degradation of ubiquitylated cyclinB (cycB) N-terminus fused with an easy-to-unfold infrared fluorescent protein iRFP (Figure 4A). We used the measured degradation rate of cycB\_NT-iRFP as an approximation for the translocation rate by the proteasomal ATPase complex, because translocating the substrate takes more than 80% of the entire turnover time, which was determined by a single-molecule translocation assay in our previous study.<sup>1</sup>

14. Ubiquitylate cycB substrates by the APC-Cdh1.
  - a. Prepare the APC ubiquitylation reaction system in the UBAB buffer containing 30 nM purified APC-Cdh1, 100 nM E1, 2  $\mu$ M UbcH10, 2 mg/mL BSA, 1  $\mu$ M substrate cycB\_NT-iRFP, 100  $\mu$ M human-ubiquitin, and 1 $\times$  E-mix.
  - b. Incubate the reaction for 4 h at 25°C.
  - c. Isolate the ubiquitylated substrates from the reaction using Dynabeads His-Tag beads following the manufacturer's instructions.
15. Prepare the proteasomal degradation reaction in 384-well plate.
  - a. Prepare pre-mix in buffer W3 on ice that contains:

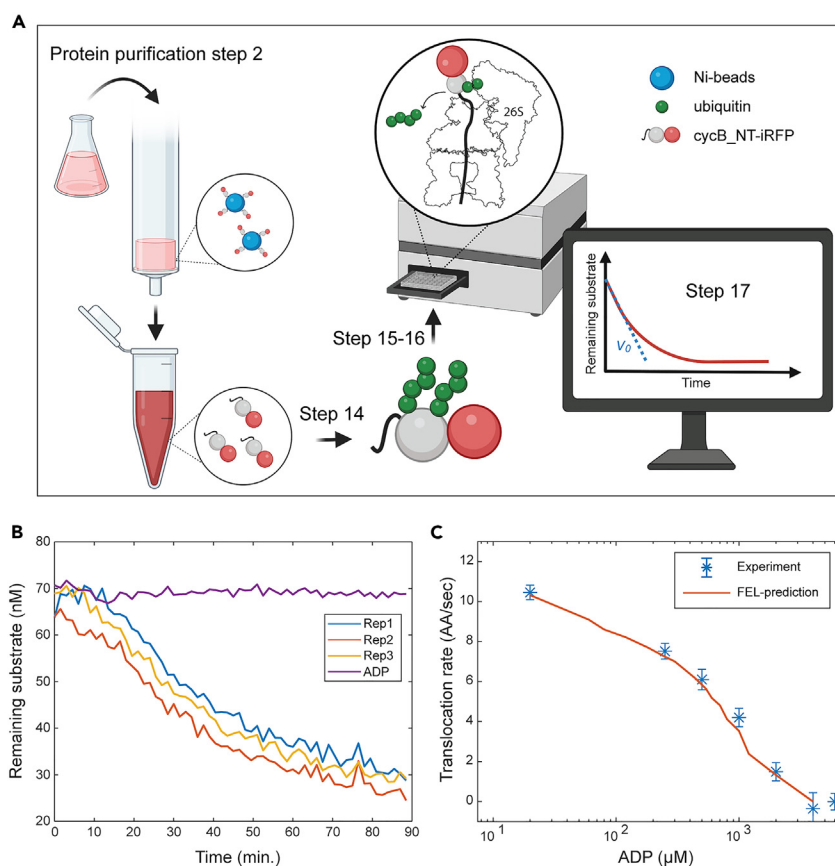


**Figure 4. The 26S proteasome activity assay**

(A) Workflow of the assay with main steps described in the section of [protein purification](#) (step 2) and the section of [the 26S proteasome activity assay](#) (steps 14, 15, 16, 17).

(B) Representative traces of the degradation of ubiquitylated cycB\_NT-iRFP by 1.5 nM purified 26S proteasome with 0.5 mM ATP (Rep 1–3) or with extra 0.8 mM ADP in the buffer. Reproduced from Fang et al.<sup>1</sup>

(C) The translocation rate of cycB\_NT-iRFP was measured using the proteasome activity assay with 0.5 mM ATP and various concentrations of ADP-Mg<sup>2+</sup>. Error bars represent the standard deviation of fifteen measurements at five substrate concentrations, each with three replicates. The red curve shows the prediction by the free-energy landscape (FEL) model. Reproduced from Fang et al.<sup>1</sup>

- i. The ubiquitylated iRFP substrates from step 14 at five concentrations: 40 nM, 60 nM, 80 nM, 120 nM, 200 nM.
  - ii. Nucleotide-Mg<sup>2+</sup> at the experimental concentrations.
- b. Aliquot the reaction to a 384-wells plate.

**Note:** For each buffer condition, the degradation assay is performed with three replicates. It is recommended to include a standard reaction with 500 μM ATP-Mg<sup>2+</sup> in every batch of reactions to control for sample batch-to-batch variations.

- c. Add purified human 26S proteasome at 1.0 nM–3.0 nM final concentration to each well of the plate.
- d. Mix slowly by pipetting with a multi-pipet.
- e. Centrifuge the plate at 1,000 × g for 1 min to eliminate bubbles and ill-formed meniscus shapes.

**Note:** Keep the plate on ice during the entire process of reaction set-up.

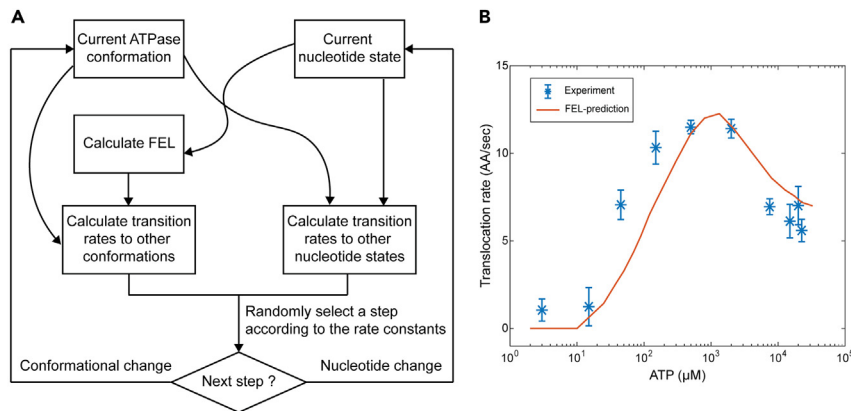


**Figure 5. Monte Carlo simulation of ATPase dynamics using the FEL model**

(A) A block diagram for simulating the dynamics of the ATPase complex using the FEL model.

(B) One example of the FEL-model predictions. The translocation rate of cycB<sub>NT</sub>-iRFP at various concentrations of ATP-Mg<sup>2+</sup> displayed a non-monotonic behavior, which is well supported by the experimental measurements (red curve). Error bars represent the standard deviation of fifteen measurements at five substrate concentrations, each with three replicates. Reproduced from Fang et al.<sup>1</sup>

16. Monitor the degradation kinetics using a microplate reader equipped with an infrared filter (EX 640/40; EM 720/10) once every 90 s at 35°C.
17. Perform linear regression to get the initial degradation rate  $v_0$  at each substrate and nucleotide concentrations from the degradation curve in the first 15 min after temperature stabilization (Figures 4A and 4B).
18. Calculate the turnover time  $1/k_{\text{cat}}$  as the inverse of the degradation rate  $v_0$  divided by the proteasome concentration based on the formula (Figure 4C):

$$v_0 = \frac{k_{\text{cat}}[26\text{S}][\text{S}]}{K_M + [\text{S}]} \sim k_{\text{cat}}[26\text{S}],$$

where  $[26\text{S}]$  is the concentration of the proteasome;  $[\text{S}]$  is the concentration of the substrate.

**Note:** The degradation of cyclinB-iRFP exhibits a Michaelis-Menten-like kinetics with  $K_M = 5.6$  nM in our original work.<sup>1</sup> All the substrate concentrations used here are much higher than the  $K_M$  to maximize the signal-to-noise ratio and to satisfy the saturation condition, and the average degradation rate of all substrate concentrations is taken as the final result.

### Monte Carlo simulation of the ATPase dynamics using the FEL model

⌚ Timing: 2 weeks

In this section, we will describe how to perform Monte Carlo simulation of the FEL model to investigate the ATPase dynamics (Figure 5A). The ATPase dynamics is simulated as stochastic transitions on its FEL in a bistate process described by the Arrhenius equation (Figure 2C). The FEL depends on the nucleotide distribution which varies according to the rate equations of the nucleotide cycle (Figure 2B). We will first describe how to set up the simulation, and then will describe how to determine the kinetic parameters listed in the section of [FEL model construction](#) using the 26S proteasome activity assay. Finally, we will present various applications of the FEL model as examples.

19. Launch MATLAB.

**Table 3. Details of elements in p1**

Variable name	Variable meaning	Default value
koff_base	$k_{on} \cdot e^{E_P/kT} \cdot C_0$	0.3333
bktrf	ratio of backward force (<0) to forward force (>0)	-0.2576
transEn	work of translocating one step (2× AAs) forward, in kcal	0.1984
tr	$k_0$	72.8000
kh_base	$k_h$	1.0340

### Single run with predetermined parameters

20. Assign the kinetic parameters with appropriate numbers in the command window:

```
>> p1 = [0.3333 -0.2576 0.1984 72.8000 1.0340];
```

**Note:** The details of five elements in p1 are listed in Table 3. The default values used for demonstration were determined by matching the simulation results with the ADP titration experiment, which will be discussed in the next section.

21. Assign the nucleotide concentrations in the command window:

```
>> nt1 = [0 0 500];
```

**Note:** Three elements in nt1 represent the concentration of ADP, ATP-γS and ATP molecules in μM. 500 μM ATP is the standard nucleotide condition in the system.

22. Run the simulation by calling the main function *FELrun* in the command window:

```
>> ret = FELrun(p1, nt1);
```

**Note:** The simulation step number is adjustable as the variable Nsteps in the script FELrun.m. We usually start with 100000. Preliminary test can be performed to make sure the ATPase complex reaches steady state after certain steps.

23. When the program finishes, save the simulation results (the structure array *ret*) in the command window with a customized filename *OutputFileName*:

```
>> save('OutputFileName.mat', 'ret');
```

**Note:** The details of the fields in the structure array ret are summarized in Table 4.

24. Get the conformational dynamics and the work output of the ATPase machine from the saved structure array *cstate*.

**Note:** The details of the fields in the structure array cstate are summarized in Table 5.

**Table 4. Details of the structure array *ret***

Field name	Field meaning
<i>N</i>	number of ATPases in the complex
<i>conATP</i>	ATP concentration in $\mu\text{M}$
<i>conADP</i>	ADP concentration in $\mu\text{M}$
<i>conATPs</i>	ATP- $\gamma\text{S}$ concentration in $\mu\text{M}$
<i>con</i>	same as input <i>nt1</i>
<i>kT</i>	product of the Boltzmann constant $k_B$ , and the temperature $T$ , in kcal/mol
<i>paraVar</i>	the maximum magnitude of the randomly drawn basal energy $e_B$
<i>bktrf</i>	from input <i>p1</i>
<i>para_e</i>	energy parameters, details in the script
<i>para_k</i>	kinetic parameters, details in the script
<i>cstate</i>	current state, details in <a href="#">Table 5</a>
<i>map</i>	mapping the index of states with conformations and nucleotide-binding status, details in the script

**Note:** \*The number of the target conformations with the lowest energy to consider can be adjusted as the variable *Nstates* in the script *evolN.m*. We usually start with 1 or 2.

#### Determine the kinetic parameters in the FEL model

- Experimentally measure the degradation rates at various ADP concentrations from 0 to 10 mM in addition to 500  $\mu\text{M}$  ATP using the 26S proteasome activity assay.
- Optimize the last four parameters in *p1* (the first one is fixed) using a gradient descent method to identify the values allowing the best match of the simulated translocation rates with experimental values at all ADP concentrations ([Figure 4C](#)).

**Note:** Remember to also change the input variable *nt1* according to the concentration of ADP used in the 26S proteasome activity assay.

#### Predict proteasome behaviors using the FEL model

A primary application of the FEL model is to understand the molecular mechanisms of the proteasome's functions that are driven by the ATPase dynamics which are inaccessible through direct experimental approaches. Here, we provide a few examples of using the FEL model to predict proteasome's behaviors and obtain mechanistic insights. We normally simulate at least 100,000 steps or until the desired property converges.

**Table 5. Details of the structure array *cstate***

Field name	Field meaning
<i>ntind</i>	current nucleotide status
<i>ifind</i>	current conformational status
<i>ntTr</i>	transition rate of the current nucleotide status to a new status
<i>cfTr</i>	transition rate of the current conformational status to new conformations with the lowest energy*
<i>cfTrind</i>	the new conformations with the lowest energy
<i>time</i>	simulated time
<i>dis</i>	total translocation distance
<i>ATPhy</i>	total ATP hydrolyzed
<i>ntM</i>	transition matrix of nucleotide status
<i>cfM</i>	transition matrix of conformational status
<i>ntV</i>	accumulating time spent at each nucleotide status
<i>cfV</i>	accumulating time spent at each conformational status



27. Predict the substrate translocation rate at a given condition. Here we take different ATP concentrations as an example (Figure 5B).
  - a. Run the simulation with various ATP concentrations from 1  $\mu$ M to 30 mM.
  - b. For each condition tested, calculate the translocation rate as `cstate.dis/ cstate.time`, where `cstate` is saved in the structure array `ret` shown in steps 23–24.
  - c. Experimentally determine the degradation rate through the 26S proteasome activity assay with the same group of ATP concentrations.
  - d. Compare the simulation results with the experimental results.
28. Predict ATP hydrolysis rate.
  - a. Run the simulation with a fixed parameter set similar as in step 27.
  - b. For each condition tested, calculate the ATP hydrolysis rate as `cstate.ATPhy/ cstate.time`.
  - c. Compare the results with experimental measurements using e.g., Malachite green assay.
29. Predict the molecular transition paths between any two states of the ATPase complex.
  - a. Set up the simulation using the starting state (conformation and nucleotide distribution) as the initial condition.
  - b. Simulate the FEL model for  $N$  steps. Stop the simulation as soon as the ATPase reaches the end state. Record the intermediate steps.
  - c. Repeat the same simulation for  $M$  times.
30. Predict the backward translocation rate of an unfolding-resistant substrate.
  - a. Predefine a peptide track length  $L_0$  which is the distance between the PL1s to the proteolytic sites inside the proteasome chamber. The substrate starts with a translocated distance  $L_0$  at  $t = 0$  when its unfolding-resistance domain is encountered by the ATPase complex, presumably its OB ring.

**Note:** We set  $L_0$  to 20–30 AAs in our practice based on the structure of the proteasome.

- b. Run the simulation with an infinite energy barrier for forward translocating the unfolding-resistance domain.
- c. The backward translocation occurs due to the stochasticity of the ATPase dynamics, without any additional assumption. The translocation process ends when the backward translocated distance is larger than  $L_0$ , when the substrate is assumed to escape from the proteasome.

**Note:** Substrate reentry is not considered due to a loss of the ubiquitin signal.

- d. The residence time of the unfolding-resistant domain on the proteasome is reported as `cstate.time`.
- e. The average backward translocation rate is calculated as `cstate.dis/ cstate.time`.
31. Predict phenotypes of ATPase mutants.
  - a. Depending on the desired mutation, set the hydrolysis rate constant of the mutated subunit to zero (Walker B mutation), or set the binding constant to zero (Walker A mutation).
  - b. Run the simulation and quantitatively evaluate the effects of the mutation on various features of the machine including the translocation rate (step 27), the ATP hydrolysis rate (step 28), and the conformational distribution which is reported as `cstate.cfV`.
32. Predict the effect of the Lid subcomplex on the ATPase dynamics.

**Note:** Based on the cryo-EM structures, the Lid subcomplex appears to only form extended interactions with the ATPase complex when the latter adopts a particular conformation as in the  $S_A$  state. We therefore make a simplifying assumption that the Lid-ATPase interaction in a  $E_A$ -like conformation stabilizes the ATPase by lowering its free energy.

- a. In the simulation, lower the standard free energy of the  $E_A$ -like conformation by 1–3 kcal/mol. Qualitatively similar results were obtained in this range.

**Note:** The value of the energy is appropriately chosen for the best consistency with experimental results used in the section of Determine the kinetic parameters in the FEL model. More details have been discussed in the previous work.<sup>1</sup> A more realistic estimation of the free-energy changes is likely to render more accurate predictions.

- b. Run the simulation with this extra energy term and quantitatively evaluate its effects on the conformational distribution reported as *cstate.cfV*.
33. Predict the global dynamical space of the proteasome, which contains the steady-state distribution of the conformations and the transition rates between each two conformations.
- a. Run the simulation till reaching the steady state at any given condition.
  - b. The steady-state distribution of the proteasomal conformations is reported as *cstate.cfV*.
  - c. The transition between each two conformations can be extracted from *cstate.cfM*.

## EXPECTED OUTCOMES

Following the above protocol, one is expected to create the FEL model for the 26S proteasome and determine its parameters. Simulating the established FEL model can yield results that guide experimental design and data analysis and help to elucidate the molecular mechanisms of proteasomal ATPases and other AAA machines which are inaccessible through direct experimental approaches. The proteasome's behaviors predicted by the FEL model include the substrate translocation rate and ATP hydrolysis rate at a given condition, the molecular transition paths between any two states of the ATPase complex, the backward translocation rate of an unfolding-resistant substrate, phenotypes of ATPase mutants, the effect of the Lid subcomplex on the ATPase dynamics, and the global dynamical space of the proteasome (details in the section of [predict proteasome behaviors using the FEL model](#)).

## LIMITATIONS

The introduction of Lid-ATPase interactions as a simple conformation-stabilizing parameter in the FEL simulation (step 32) recapitulates the asymmetric cryo-EM state distributions and may explain the different phenotypes of WB mutants that were discussed thoroughly in the previous work.<sup>1</sup> Including the Lid-ATPase interaction in the model yields predictions that are compatible with all the kinetic measurements in our study and indicates that the proteasome may occasionally visit an  $E_A$ -like state during translocation.<sup>24</sup> However, the peak translocation rate is underestimated by 20%–25% in this case, suggesting that our understanding of the symmetry-breaking mechanism is still incomplete.

The FEL model focuses on the translocation process. Currently, this model may not accurately describe the degradation of substrates which are limited by steps other than translocation. Extending the FEL model to cover other ATPase-driven processes on proteasome may provide further insights into the mechanism of proteasomal degradation. Moreover, the current FEL model assumes no explicit allosteric effects. Although this simplification does not appear to affect accuracy of the predictions in our previous study, allosteric communications, such as the ones between the substrate peptide and the nucleotide pockets,<sup>15</sup> are likely to exist on proteasome, and may provide additional flexibility to the control of proteasome activities.

Although the simulation recapitulates important properties of the proteasome, the empirical FEL is undoubtedly an approximation of the actual FEL of the proteasome. Studies, such as the one by Saha et al.,<sup>25</sup> which determined the free-energy contribution by the substrate-proteasome interaction, can be incorporated to increase the accuracy of the FEL-based simulation.

## TROUBLESHOOTING

### Problem 1

Nonspecific binding of the passivated coverslips is high (step 8).

#### Potential solution

- Replace all reagents with freshly opened or freshly prepared ones, especially DDS which easily hydrolyzes at 20°C–25°C. Check the fluorescent signal of each reagent used in step 8 to make sure all reagents except for the dye solutions have no autofluorescence or fluorescent contaminants.
- Rinse the coverslips extensively in step 6 and make sure to damp all water completely after each wash.

### Problem 2

Binding capacity of the 26S proteasome on the image surface is low (steps 10–11).

#### Potential solution

- Repeat step 8 to titrate for the best protein concentration to use using the avidin-rhodamine solution.
- Another possible explanation is the disassembly of the 26S holoenzyme into 19S and 20S particles during steps 9–10. To reduce the rate of disassembly, the proteasome sample should be prepared as quickly as possible and always kept on ice.

**Note:** We have a stable HEK293-Rpn11-HTBH cells with pCMV- $\beta$ 1-FLAG-SNAP (HEK293- $\beta$ 1-SNAP) to purify 26S proteasomes with a SNAP-tagged 20S. The disassembly rate can be estimated through comparing the binding capacity of Rpn3-tagged proteasome and  $\beta$ 1-tagged proteasome.

### Problem 3

Large fluctuations of the degradation curve (steps 16–17).

#### Potential solution

- If the large fluctuations show up at the beginning of the degradation curve, it is mostly likely caused by the temperature shift right after putting the 4°C plate into the microplate reader set to 35°C. Only keep time points after the temperature becomes stable to perform linear regression.
- If the big fluctuations show up in the middle of the degradation curve, it is mostly likely caused by bubbles in the well. We recommend discarding the data from that well. Pipetting slowly and spin the plate at 1,000  $\times$  g for 1 min right before incubation could help to reduce the incidence of bubbles.
- Repeat each condition for at least 3 times to reduce random noise and accidents mentioned above.

### Problem 4

Simulation results are not saved (steps 22–23).

#### Potential solution

- Make sure that the program finishes normally after which the notification “**finished test...**” will be displayed in the command window. If you see neither the notification nor “**Busy**” at the lower bar of the MATLAB main window, MATLAB might stop responding due to the large simulation step number *Nsteps*. Try to start with a smaller *Nsteps* like 1000.

- Make sure that the results of the function *FELrun* are returned to a variable (e.g., *ret* in step 22) when you call the function:

```
>> ret = FELrun(p1, nt1);
```

No results will be returned if you just call the function as:

```
>> FELrun(p1, nt1);
```

- Lastly, make sure you assign a new file name in step 23 for each new run to avoid overwriting.

### Problem 5

The parameters in *p1* cannot be optimized to values allowing a good match of the simulated translocation rates with experimental values (step 26). An example of a “good” match is shown in Figure 4C.

### Potential solution

The initial values might be too far from the optimal values or the step size in the gradient descent method might be too large.

- We recommend starting with values that are biologically relevant based on previously published experimental data.
- To increase efficiency in the optimization, we recommend adapting the code *FELrun.m* for parallel computing using Parallel Computing Toolbox in MATLAB. Codes are available upon request.

## RESOURCE AVAILABILITY

### Lead contact

Further information and requests for resources and reagents should be directed to and will be fulfilled by the lead contact, Ying Lu ([ying\\_lu@hms.harvard.edu](mailto:ying_lu@hms.harvard.edu)).

### Materials availability

All plasmids and cell lines mentioned in this study are available from the [lead contact](#) upon request.

### Data and code availability

All original code can be downloaded following instructions in the section of [install software and download the source code](#). The parallel version of the FEL model algorithm is available from the [lead contact](#) upon request. Data generated from this study are available from the [lead contact](#) upon request.

Proteasome FEL model algorithm: <https://doi.org/10.5281/zenodo.7637421>.

Proteasome structure analysis package: <https://doi.org/10.5281/zenodo.7618588>.

## ACKNOWLEDGMENTS

The authors thank L Huang for sharing constructs for proteasome purification and thank B Schulman and N Brown for sharing constructs for APC/C purification. The authors are grateful for the critical reading and comments by M Kirschner, Y Tu, T Mitchison, D Finley, A Goldberg, L Bai, R Ward, J Yan, and P Ho. Portions of this research were conducted on the O2 High Performance Compute Cluster, supported by the Research Computing Group, at Harvard Medical School. This work is

supported by an NIH R01 Grant to Y.L. (GM134064-01), an Edward Mallinckrodt, Jr foundation award to Y.L., and a Harvard Medical School Dean's Initiative award to R.F. and Y.L.

## AUTHOR CONTRIBUTIONS

Conceptualization, R.F., Y.L.; Data curation, R.F., Y.L.; Formal analysis, R.F., Y.L.; Investigation, R.F., Y.L.; Software, R.F., Y.L.; Validation, R.F., Y.L.; Visualization, R.F., Y.L.; Writing - original draft, R.F., Y.L.; Writing - review and editing, R.F., Y.L.; Funding acquisition, Y.L.; Methodology, Y.L.; Project administration, Y.L.; Resources, Y.L.; Supervision, Y.L.

## DECLARATION OF INTERESTS

The authors declare no competing interests.

## REFERENCES

- Fang, R., Hon, J., Zhou, M., and Lu, Y. (2022). An empirical energy landscape reveals mechanism of proteasome in polypeptide translocation. *Elife* 11, e71911. <https://doi.org/10.7554/eLife.71911>.
- Erzberger, J.P., and Berger, J.M. (2006). Evolutionary relationships and structural mechanisms of AAA+ proteins. *Annu. Rev. Biophys. Biomol. Struct.* 35, 93–114. <https://doi.org/10.1146/annurev.biophys.35.040405.101933>.
- Puchades, C., Sandate, C.R., and Lander, G.C. (2020). The molecular principles governing the activity and functional diversity of AAA+ proteins. *Nat. Rev. Mol. Cell Biol.* 21, 43–58. <https://doi.org/10.1038/s41580-019-0183-6>.
- White, S.R., and Lauring, B. (2007). AAA+ ATPases: achieving diversity of function with conserved machinery. *Traffic* 8, 1657–1667. <https://doi.org/10.1111/j.1600-0854.2007.00642.x>.
- Collins, G.A., and Goldberg, A.L. (2017). The logic of the 26S proteasome. *Cell* 169, 792–806. <https://doi.org/10.1016/j.cell.2017.04.023>.
- Bard, J.A.M., Goodall, E.A., Greene, E.R., Jonsson, E., Dong, K.C., and Martin, A. (2018). Structure and function of the 26S proteasome. *Annu. Rev. Biochem.* 87, 697–724. <https://doi.org/10.1146/annurev-biochem-062917-011931>.
- Koga, N., and Takada, S. (2006). Folding-based molecular simulations reveal mechanisms of the rotary motor F1-ATPase. *Proc. Natl. Acad. Sci. USA* 103, 5367–5372. <https://doi.org/10.1073/pnas.0509642103>.
- Kravats, A.N., Tonddast-Navaei, S., and Stan, G. (2016). Coarse-grained simulations of topology-dependent mechanisms of protein unfolding and translocation mediated by ClpY ATPase nanomachines. *PLoS Comput. Biol.* 12, e1004675. <https://doi.org/10.1371/journal.pcbi.1004675>.
- Kmiecik, S., Gront, D., Kolinski, M., Wieteska, L., Dawid, A.E., and Kolinski, A. (2016). Coarse-grained protein models and their applications. *Chem. Rev.* 116, 7898–7936.
- Shaw, D.E., Adams, P.J., Azaria, A., Bank, J.A., Batson, B., Bell, A., Bergdorf, M., Bhatt, J., Butts, J.A., and Correia, T. (2021). Anton 3: twenty microseconds of molecular dynamics simulation before lunch. In *SC21: International Conference for High Performance Computing, Networking, Storage and Analysis (IEEE)*, pp. 1–11.
- Weissmann, F., Petzold, G., VanderLinden, R., Huis In 't Veld, P.J., Brown, N.G., Lampert, F., Westermann, S., Stark, H., Schulman, B.A., and Peters, J.M. (2016). biGBac enables rapid gene assembly for the expression of large multisubunit protein complexes. *Proc. Natl. Acad. Sci. USA* 113, E2564–E2569. <https://doi.org/10.1073/pnas.1604935113>.
- Jarvis, M.A., Brown, N.G., Watson, E.R., VanderLinden, R., Schulman, B.A., and Peters, J.M. (2016). Measuring APC/C-dependent ubiquitylation in vitro. *Methods Mol. Biol.* 1342, 287–303. [https://doi.org/10.1007/978-1-4939-2957-3\\_18](https://doi.org/10.1007/978-1-4939-2957-3_18).
- Brown, N.G., VanderLinden, R., Watson, E.R., Weissmann, F., Ordureau, A., Wu, K.P., Zhang, W., Yu, S., Mercredi, P.Y., Harrison, J.S., et al. (2016). Dual RING E3 architectures regulate multiubiquitination and ubiquitin chain elongation by APC/C. *Cell* 165, 1440–1453. <https://doi.org/10.1016/j.cell.2016.05.037>.
- Wang, X., Chen, C.F., Baker, P.R., Chen, P.L., Kaiser, P., and Huang, L. (2007). Mass spectrometric characterization of the affinity-purified human 26S proteasome complex. *Biochemistry* 46, 3553–3565. <https://doi.org/10.1021/bi061994u>.
- Dong, Y., Zhang, S., Wu, Z., Li, X., Wang, W.L., Zhu, Y., Stoilova-McPhie, S., Lu, Y., Finley, D., and Mao, Y. (2019). Cryo-EM structures and dynamics of substrate-engaged human 26S proteasome. *Nature* 565, 49–55. <https://doi.org/10.1038/s41586-018-0736-4>.
- Al-Shawi, M.K., and Nakamoto, R.K. (1997). Mechanism of energy coupling in the FOF1-ATP synthase: the uncoupling mutation, gammaM23K, disrupts the use of binding energy to drive catalysis. *Biochemistry* 36, 12954–12960. <https://doi.org/10.1021/bi971477z>.
- de la Peña, A.H., Goodall, E.A., Gates, S.N., Lander, G.C., and Martin, A. (2018). Substrate-engaged 26S proteasome structures reveal mechanisms for ATP-hydrolysis-driven translocation. *Science* 362, eaav0725. <https://doi.org/10.1126/science.aav0725>.
- Majumder, P., Rudack, T., Beck, F., Danev, R., Pfeifer, G., Nagy, I., and Baumeister, W. (2019). Cryo-EM structures of the archaeal PAN-proteasome reveal an around-the-ring ATPase cycle. *Proc. Natl. Acad. Sci. USA* 116, 534–539. <https://doi.org/10.1073/pnas.1817752116>.
- Kim, Y.C., Snoberger, A., Schupp, J., and Smith, D.M. (2015). ATP binding to neighbouring subunits and intersubunit allosteric coupling underlie proteasomal ATPase function. *Nat. Commun.* 6, 8520. <https://doi.org/10.1038/ncomms9520>.
- Eisele, M.R., Reed, R.G., Rudack, T., Schweitzer, A., Beck, F., Nagy, I., Pfeifer, G., Plitzko, J.M., Baumeister, W., Tomko, R.J., Jr., and Sakata, E. (2018). Expanded coverage of the 26S proteasome conformational landscape reveals mechanisms of peptidase gating. *Cell Rep.* 24, 1301–1315.e5. <https://doi.org/10.1016/j.celrep.2018.07.004>.
- Smith, D.M., Fraga, H., Reis, C., Kafri, G., and Goldberg, A.L. (2011). ATP binds to proteasomal ATPases in pairs with distinct functional effects, implying an ordered reaction cycle. *Cell* 144, 526–538. <https://doi.org/10.1016/j.cell.2011.02.005>.
- Peth, A., Nathan, J.A., and Goldberg, A.L. (2013). The ATP costs and time required to degrade ubiquitinated proteins by the 26 S proteasome. *J. Biol. Chem.* 288, 29215–29222. <https://doi.org/10.1074/jbc.M113.482570>.
- Hon, J., and Lu, Y. (2019). Single-molecule methods for measuring ubiquitination and protein stability. *Methods Enzymol.* 619, 225–247. <https://doi.org/10.1016/bs.mie.2018.12.031>.
- Jonsson, E., Htet, Z.M., Bard, J.A.M., Dong, K.C., and Martin, A. (2022). Ubiquitin modulates 26S proteasome conformational dynamics and promotes substrate degradation. *Sci. Adv.* 8, eadd9520. <https://doi.org/10.1126/sciadv.add9520>.
- Saha, A., and Warshel, A. (2021). Simulating the directional translocation of a substrate by the AAA+ motor in the 26S proteasome. *Proc. Natl. Acad. Sci. USA* 118, e2104245118. <https://doi.org/10.1073/pnas.2104245118>.